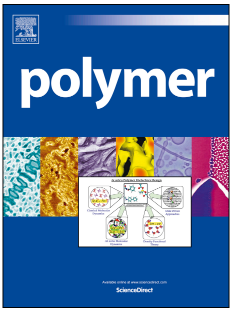

Regioisomeric π-conjugated terpolymers bearing carboxylate substituted thienothiophenyl quarterthiophene and their application to fullerene-free polymer solar cells

Chang Geun Park, Gi Eun Park, Ji Hyung Lee, Aesun Kim, Young Un Kim, Seo Yeon Park, Su Hong Park, Min Ju Cho, Dong Hoon Choi

PII: S0032-3861(18)30423-3

DOI: 10.1016/j.polymer.2018.05.027

Reference: JPOL 20588

To appear in: *Polymer*

Received Date: 26 February 2018

Revised Date: 24 April 2018

Accepted Date: 8 May 2018

Please cite this article as: Park CG, Park GE, Lee JH, Kim A, Kim YU, Park SY, Park SH, Cho MJ, Choi DH, Regioisomeric π-conjugated terpolymers bearing carboxylate substituted thienothiophenyl quarterthiophene and their application to fullerene-free polymer solar cells, *Polymer* (2018), doi: 10.1016/j.polymer.2018.05.027.

TOC

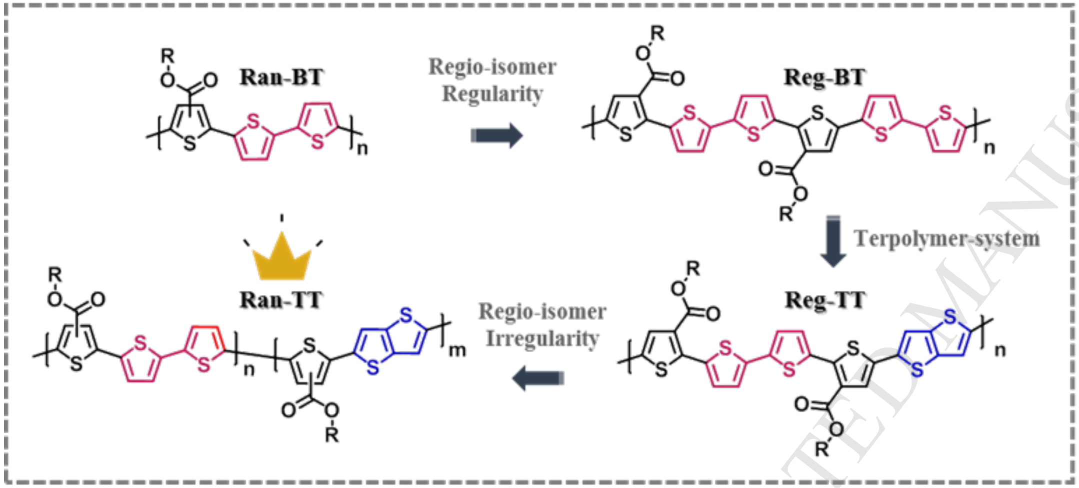
Ran-BT
Regio-isomer
Regularity
Reg-BT
Terpolymer-system
Ran-TT
Regio-isomer
Irregularity
Reg-TT
R
O
O
S
n
m

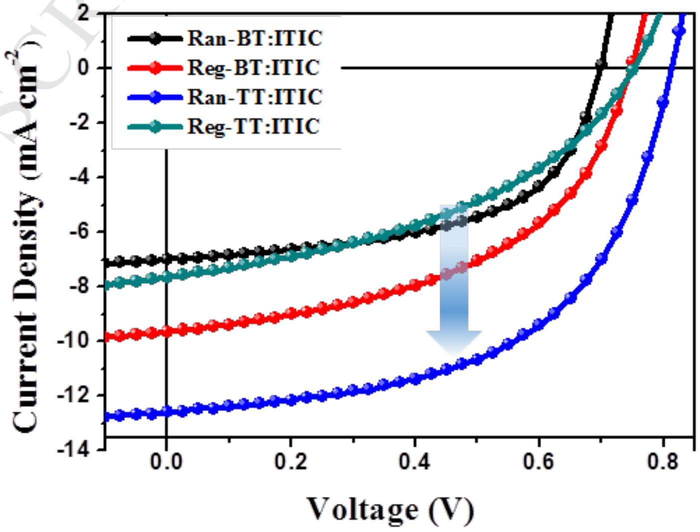
Ran-BT:ITIC
Reg-BT:ITIC
Ran-TT:ITIC
Reg-TT:ITIC
Current Density (mA cm^{-2})
Voltage (V)
2
0
-2
-4
-6
-8
-10
-12
-14
0.0
0.2
0.4
0.6
0.8

Regioisomeric π-Conjugated Terpolymers bearing Carboxylate substituted Thienothiophenyl Quarterthiophene and Their Application to Fullerene-free Polymer Solar Cells

Chang Geun Park [a], Gi Eun Park [a,b], Ji Hyung Lee [a], Aesun Kim [a], Young Un Kim [a], Seo Yeon Park [a], Su Hong Park [a], Min Ju Cho [a,*] and Dong Hoon Choi [a.*]

[a] Department of Chemistry, Research Institute for Natural Sciences, Korea University, 145 Anam-Ro, Sungbuk-gu, Seoul 02841, Republic of Korea

[b] Photo-electronic Hybrids Research Center, Korea Institute of Science and Technology, Seoul 02792, Republic of Korea

Abstract

Two regioisomeric π-conjugated terpolymers bearing carboxylated thiophene (CT) as electron accepting unit and thienothiophene (TT) and bithiophene (BT) as electron donating units were successfully synthesized for enhancing the performance of polymer solar cells (PSCs). Regio-regular and regio-random binary copolymers based on CT and BT were also prepared as control polymers. All polymers showed unique optical properties and crystalline behaviors. Among the PSC devices fabricated in this study, the PSC based on the regio-random terpolymer (**Ran-TT**) and 3,9-bis(2-methylene-(3-(1,1-dicyanomethylene)-indanone))-5,5,11,11-tetrakis(4-hexylphenyl) dithieno[2,3-*d*:2′,3′-*d*′]-s-indaceno[1,2-*b*:5,6*b*′]-dithiophene (ITIC) exhibited the highest power conversion efficiency of 5.65% with a high short circuit current density (J_{sc}) of 12.63 mA cm^{-2} and an open circuit voltage (V_{oc}) of 0.81 V. The promising PCE value is attributed to the low-lying highest occupied molecular orbital (HOMO) of **Ran-TT**, effective complementary absorption spectrum and favorable internal morphology of the blend film. The internal morphology of the **Ran-TT** was observed to be more fine phase separation than that of the regio-regular terpolymer, facilitating exciton diffusion and dissociation in the bulk heterojunction.

Keywords: carboxylated thiophene, regioisomeric, terpolymer, organic solar cell, semiconductor

Correspondence to: M. J. Cho (chominju@korea.ac.kr) and D. H. Choi (E-mail: dhchoi8803@korea.ac.kr)

Introduction

Polymer solar cells (PSCs) have been studied intensively due to the excellent film-forming ability, persistent internal morphology, desirable thin film structure, high light absorptivity, and mechanical flexibility of the conjugated polymers composing the active layer.[1-4]

The most commonly known PSCs include bulk heterojunctions (BHJs) with an active layer composed of a conjugated polymer as an electron donor and a low molecular weight compound or polymer as an electron acceptor. In the early study of BHJ-type PSC, fullerene derivatives such as [6,6]-phenyl-(C_{61} or C_{71})-butyric acid methyl ester ($PC_{61}BM$ or $PC_{71}BM$), which exhibit electron-withdrawing ability, were mainly used as acceptor materials. However, the inflexibility of the molecular structure, low absorption in the visible light region, and self-associating characteristics have been pointed out as disadvantages in enhacing the efficiency of PSC.[5,6] To overcome these drawbacks, a number of studies were recently conducted on non-fullerene acceptors. For example, materials such as perylenediimide (PDI) derivatives, naphthalene diimide (NDI) derivatives, and indaceno-dithiophene (IDT)-based small molecules have been employed for fabricating high-performing PSCs.[7-10] To achieve efficient complementary absorption behavior with blend films containing the new non-fullerene acceptors described above, new donor polymers with a wide bandgap energy and strong absorption in the short wavelength region need to be developed.[11,12]

Recently, high-performing wide-bandgap donor polymers bearing donor(D) and acceptor(A) moieties in the repeating group have been utilized to fabricate high-efficiency non-fullerene PSCs .[13-18] On the other hand, polythiophene (PT) derivatives with wide bandgap energies have previously been used as donor polymers due to their accessibility and ease of synthesis. However, PT derivatives have a relatively high-lying HOMO level and a resulting low open circuit voltage (V_{oc}), which is directly related to the gap between the HOMO of the donor and the LUMO of the acceptor, making it difficult to implement these molecules in PSCs. To remedy this problem, extensive efforts have been devoted to developing new PT derivatives by employing more effective conjugative units to tune their energy levels and modify the morphology of the blend film with the acceptors. For instance, Hou et al. demonstrated that the PT derivative P3HDTTT allowed for a relatively low-lying HOMO level (E_{HOMO} = -5.3 eV) by reducing the number of alkyl groups and reducing the electron donating effect. Using this approach, the V_{oc} was increased from 0.64 V to 0.82 V.[13]

Many attempts have been made to introduce carboxylates into the thiophene unit, as well as to employ side-chain engineering by modifying the alkyl chain. This approach has been shown to reduce the HOMO level without significantly changing the optical bandgap. Zang et al. developed a series of PT derivatives (e.g. PT-C1, PT-C2 and PT-C3) containing carboxylate substituents and the PSC based on PT-C3 having the largest branched alkyl side chain, showed improved V_{oc} of 0.78 V, which is higher than the PSC made with P3HT (V_{oc} = 0.60 V), having no carboxylates.[19]

As noted above, most previous studies have focused on tuning the energy level of the PT polymer. To further improve the efficiency of the BHJ-type PSC, studies on improving the internal morphology of the blend films with non-fullerene acceptors should be performed. An effective design strategy to obtain a favorable blend film morphology is to control the regio-regularity of the donor polymer backbone structure. The effect of regio-random and regio-regular conjugated donor polymer structures on the performance of PSC devices using high performance acceptors has been studied.[20-28]

Most recently, a number of studies have been conducted on conjugated terpolymer as one useful method for precisely manipulating the physical properties of binary D-A copolymers. By introducing a new third conjugated monomer, the resulting polymer properties such as the spectral absorption, charge transport, solubility, and blend film morphology can be finely controlled compared to conventional binary copolymers.

In this study, we proposed conjugated terpolymers by employing regio-random and regio-regular polythiophene derivatives with a carboxylate side chain and further introducing thienothiophene as a third monomer. Thus, new asymmetric carboxylate substituted PT-based terpolymers, **Ran-TT** and **Reg-TT**, were successfully synthesized herein, along with PT-C3(**Ran-BT)** and **Reg-BT** as control polymers. Eventually, they were employed to fabricate inverted type PSCs for their comparison. The blend film of 3,9-bis(2-methylene-(3-(1,1-dicyanomethylene)-indanone))-5,5,11,11-tetrakis(4-hexylphenyl) dithieno[2,3-*d*:2′,3′-*d*′]-s-indaceno[1,2-*b*:5,6*b*′]-dithiophene (ITIC) and **Reg-TT** exhibits poor photovoltaic performance with a PCE of 2.43%. To modulate the performance of the PSC based on **Reg-TT**, we also employ the random terpolymer **Ran-TT** in corresponding PSCs, where the terpolymer displays an fine internal morphology with ITIC in the blend film state. The fully optimized **Ran-TT**:ITIC based device provides the highest PCE of over 5.65% with a high J_{sc} of 12.57 mA cm^{-2}. Compared with the PSC performance achieved using **Ran-BT**, **Ran-TT**-based PSC provides a significantly enhanced PCE.

Experimental

Materials

The chemicals required to synthesize the polymers used in this study were purchased from Sigma-Aldrich, Acros Organics, and Tokyo Chemical Industry and were used without further purification. Compounds **2**, **3**, **4**, **M3**, and **M4** were synthesized according to published methods.[29−32]

Synthesis of monomers and polymers

2,5-Dibromothiophene-3-carboxylic acid (2).

Compound **1** (2.00 g, 15.6 mmol) was dissolved in glacial acetic acid (25.0 mL) and Br_2 (12.4 g, 78.0 mmol) was added to the above solution dropwise at room temperature. The mixture was heated and stirred at 60 °C for 24 h. After the reaction was completed, the mixture was poured into 200 mL of deionized water to quench the reaction. The precipitate was filtered and dissolved in ethyl acetate (EA). The solution in EA was dried with Na_2SO_4. After evaporation of the solvent, the crude product was purified by recrystallization from EtOH−H_2O to give the product as a white powder (3.60 g, yield 80.7%; ^{1}H NMR (500 MHz, $CDCl_3$; δ (ppm)): 13.29 (s, 1H), 7.44 (s, 1H)).

2-Hexyldecyl 2,5-dibromothiophene-3-carboxylate (3).

A mixture of compound **2** (2.50 g, 8.74 mmol) and K_2CO_3 (3.63 g, 9.62 mmol) was dissolved in dimethyl formamide (DMF; 20.0 mL). The mixture was stirred for 1 h under Ar atmosphere and 1-iodo-2-hexyldecane (2.60 g, 9.62 mmol) was added and stirred overnight. Deionized water (50.0 mL) with a small amount of 1 M HCl (2−3 mL) was poured into the mixture to quench the reaction, followed by extraction with CH_2Cl_2. The organic phase was dried with Na_2SO_4 and the solvent was removed in vacuo. The product was purified by column chromatography on silica gel using hexane/CH_2Cl_2 (4:1 v/v), yielding the pure compound as a colorless oil (1.70 g, yield 38.0%; ^{1}H NMR (500 MHz, $CDCl_3$; δ (ppm)): 7.33(s, 1H), 4.19–4.18 (d, J = 5.8 Hz, 2H), 1.74–1.71 (m, 1H), 1.42–1.27 (m, 14H), 0.89–0.86 (m, 6H)).

2-Bromothiophene-3-carboxylic acid (4).

An oven-dried 100 mL round bottom flask was charged with compound **1** (2.00 g, 15.6 mmol) and tetrahydrofuran (THF; 30 mL). The solution was cooled to -78.0 ^{o}C and 2.50 M *n*-butyllithium in hexane (12.6 mL, 31.5 mmol) was slowly added dropwise. The reaction mixture was stirred for 30 min at -78.0 ^{o}C and bromine (0.86 mL, 16.4 mmol) was added dropwise. Stirring was continued for 1 h at -78.0 ^{o}C and the mixture was heated to room temperature. After stirring the mixture overnight, a small amount of dilute 1 M HCl (50.0 mL) was added to quench the reaction and the solution was then concentrated. After extracting the resultant mixture using ether and water, the organic layer was dried with Na_2SO_4. The compound was recrystallized twice using a H_2O/ether mixture to furnish the compound as faint yellow needles (2.13 g, yield 66.0%; ^{1}H NMR (500 MHz, DMSO-d_6, δ (ppm)): 7.63−7.62 (d, *J* = 5.8 Hz, 1H), 7.32−7.31 (d, *J* = 5.8 Hz, 1H)).

2-Hexyldecyl 2-bromothiophene-3-carboxylate (5).

A mixture of compound **4** (2.10 g, 10.1 mmol) and K_2CO_3 (4.21 g, 30.4 mmol) was dissolved in DMF (15.0 mL). The mixture was stirred for 1 h under argon atmosphere; 1-iodo-2-hexyldecane (3.93 g, 11.2 mmol) was added and stirred overnight. After the reaction was completed, the mixture was poured into 50 mL of deionized water and a small amount of 1 M HCl (3−5 mL) was added to quench the reaction, followed by extraction with CH_2Cl_2. The organic phase was dried with Na_2SO_4 and the solvent was removed. The product was purified via column chromatography on silica gel using hexane/CH_2Cl_2 (4:1), yielding the pure compound as a colorless oil (3.00 g, yield 68.5%; ^{1}H NMR (500 MHz, $CDCl_3$, δ(ppm)): 7.37−7.36 (d, *J* = 5.8 Hz, 1H), 7.23−7.21 (d, *J* = 5.8 Hz, 1H), 4.21−4.20 (d, *J* = 5.5 Hz, 2H), 1.76−1.73 (m, 1H), 1.45−1.27 (m, 24H), 0.89−0.86 (m, 6H)).

Bis(2-hexyldecyl)-[2,2':5',2'':5'',2'''-quaterthiophene]-3,3'''di-carboxylate (6).

Compound **5** (1.50 g, 3.50 mmol) and 5,5'-bis(trimethylstann-yl)-2,2'-bithiophene (0.85 g, 1.70 mmol) were dissolved in toluene (18.0 mL) and dimethylformamide (DMF) (2.00 mL). The reaction mixture was degassed with argon, after which tris(dibenzylideneacetone)dipalladium ($Pd_2(dba)_3$) (80.0 mg, 5 mol%) and tri(o-tolyl)phosphine (P(*o*-tolyl)$_3$) (53.0 mg, 5 mol%) were added to the mother mixture.

The mixture was heated to 110 °C and continuously stirred for 24 h. After the reaction was completed, the mixture was poured into 50.0 mL of deionized water and then extracted with CH_2Cl_2. The organic phase was dried with Na_2SO_4 and the solvent was removed. The product was purified via column chromatography on silica gel using hexane/CH_2Cl_2 (1.5:1), yielding the pure compound as a light yellow oil (1.0 g, yield 66.7%).; ^{1}H NMR (500 MHz, $CDCl_3$, δ(ppm)): 7.49−7.48 (d, *J* = 5.5 Hz, 2H), 7.39−7.38 (d, *J* = 4.0 Hz, 2H), 7.20−7.19 (d, *J* = 5.8 Hz, 2H), 7.16 (d, *J* = 3.7 Hz, 2H), 4.17−4.16 (d, *J* = 5.8 Hz, 4H), 1.69 (m, 2H), 1.29−1.24 (m, 48H), 0.88−0.85 (m, 12H). ; MALDI-TOF: m/z = 866.13

Bis(2-hexyldecyl) 5,5'''-dibromo-[2,2':5',2'':5'',2'''-quaterthio-phene]-3,3'''dicar-boxylate (7).

Compound **6** (1.00 g, 1.20 mmol) and *N*-bromosuccinimide (NBS) (0.41 g, 2.30 mmol) were dissolved in chloroform (5.00 mL) and acetic acid (5.00 mL). The mixture was stirred for 24 h at room temperature. After the reaction was finished, the mixture was poured into 50.0 mL of deionized water and then extracted with hexane/ether to remove the acid completely. The product was purified by column chromatography on silica gel using hexane/CH_2Cl_2 (2:1), yielding the pure compound as a yellow oil (0.60 g, yield 50.9%).; ^{1}H NMR (500 MHz, $CDCl_3$, δ(ppm)): 7.42 (s, 2H), 7.33 (d, *J* = 4.0 Hz, 2H), 7.15 (d, *J* = 4.0 Hz, 2H), 4.15−4.14 (d, *J* = 5.5 Hz, 4H), 1.68 (m, 2H), 1.28−1.25 (m, 48H), 0.88−0.87 (m, 12H). MALDI-TOF: m/z = 1025.27

Polymerization.

All four polymers were synthesized by the Stille coupling reaction. **Ran-BT** and **Reg-BT** were prepared by using the monomer (1 equiv). 5,5'-Bis(trimethylstannyl)-2,2'-bithiophene (1 equiv), $Pd_2(dba)_3$, and P(*o*-tolyl)$_3$ were added to a 2-neck round bottom flask. Dry toluene (10 mL) was then added and the mixture was degassed. Compound **3** was stirred and refluxed for 24 h at 110 ^oC (**Ran-BT**) and **7** was reacted in dry toluene (50 mL) under dilute conditions for 5 h at 110 ^oC (**Reg-BT**). **Ran-TT** and **Reg-TT** were prepared by using the monomers (1 equiv); 5,5'-bis(trimethylstannyl)-2,2'-bithiophene (1 equiv) and 2,5-bis(trimethylstannyl)thieno[3,2-b]thiophene (1 equiv) were added to a 2-neck round bottom flask in the presence of $Pd_2(dba)_3$ and P(*o*-tolyl)$_3$. Dry toluene (50 mL) was added and the mixture was degassed with argon. **Ran-TT** and **Reg-TT** were prepared under reflux for 48 h at 110 ^oC and 5 h at 110 ^oC, respectively. After cooling to room temperature, the resulting solution was precipitated into methanol (300 mL). To remove the by-products and oligomers, Soxhlet extraction was conducted with acetone, n-hexane, methyl chloride, and chloroform successively. The chloroform fraction was then precipitated into methanol (300 mL) and dried under vacuum at 40 ^oC for 24 h. (**Ran-BT** M_n = 12.3 kDa, PDI = 1.86; **Reg-BT** M_n = 32.4 kDa, PDI = 1.97; **Ran-TT** M_n = 33.8 kDa, PDI = 2.01; **Reg-TT** M_n = 23.5 kDa, PDI = 2.24).

Instrumentation

The ^1H NMR spectra of all the compounds were analyzed by using a Bruker 500 MHz spectrometer (Ascend 500, Bruker). The absorption spectra of the small molecules and polymers in chloroform solution and thin films were recorded using a UV−vis absorption spectrometer (Agilent 8453, photodiode array, λ = 190−1100 nm). The electrochemical properties were character-ized by cyclic voltammetry (CV, eDAQ EA161) with an electrolyte solution comprising tetrabutylammonium hexafluorophosphate (Bu_4NPF_6) in acetonitrile. A platinum wire and Ag/AgCl were used as the counter and reference electrodes, respectively. The number average molecular weight (M_n) and polydispersity index (PDI) of the polymers were measured relative to polystyrene (PS) standards by gel permeation chromatography (GPC) with chloroform as the eluent using an Agilent GPC 1200 series instrument. Grazing incidence wide-angle X-ray diffraction (GIWAXD) measurements were conducted at the 9A (U-SAXS) beamline (energy = 11.05 keV, pixel size = 79.59 μm, wavelength (λ) = 1.12199 Å, 2θ = 0−20°) of the Pohang Accelerator Laboratory (PAL). Samples were prepared by spin-coating the molecule solutions onto a SiO_2 wafer. The surface morphologies of the films were explored using an atomic force microscope (XE-100, Advanced Scanning Probe Microscope, PSIA) with a silicon cantilever. The morphology of each polymer film surface was investigated by atomic force microscopy (AFM; Advanced Scanning Probe Microscope, XE-100, PSIA). Transmission electron microscopy (TEM) imaging was performed using a Tecnai G2F30 transmission electron microscope (FEI Inc.; accelerating voltage = 300 kV).

Fabrication of Polymer Solar Cell

Inverted solar cells were fabricated with the ITO (150 nm)/ZnO (30 nm)/polymer:ITIC /MoO_3 (10 nm)/Ag (100 nm) configuration. The pre-patterned ITO glass (150 nm, R = 10.0 Ω cm^{-2}) was washed with acetone, deionized water, and isopropyl alcohol for 10 min each in the stated order. A ZnO layer was spin-coated on the washed ITO glass at 3000 rpm for 40 s after UV-ozone processing for 20 min and then annealed at 165 °C for 1 h. The substrates were then transferred into a N_2 protected glove box. The polymer:ITIC blends were obtained by spin coating the chloroform solution (1.0 wt%) with a 1:1 weight ratio of the polymer and ITIC. The blend solutions were stirred overnight at 60 °C and spin coated onto an ITO/ZnO substrate at 3000 rpm for 40 s. Then, the spin coated films was annealed at 100 ^{o}C for 10 min. Finally, MoO_3 (10 nm) and Ag (100 nm) were deposited on the photoactive layer by thermal evaporation. The current density−voltage ($J-V$) characteristics were measured by using a Keithley 2400 source meter under AM 1.5 G illumination at 100 mW cm^{-2} (Oriel, 1000 W). The incident light intensity was measured by using a calibrated broadband optical power meter (Spectra Physics, model 404). EQE spectra were recorded with a K3100 EQX instrument with a K240 XE300 lamp source. The optimized device is illustrated in **Fig. S1**.

Space-charge-limited current (SCLC) method for measuring charge carrier mobility

The structures of the hole only devices (HODs) and electron only devices (EODs) were ITO/PEDOT:PSS/active layer/Au and ITO/ZnO/active layer/LiF/Al, respectively. Each active layer was fabricated using the optimum conditions described for the PSCs. The thickness of the active layers was adjusted to be 110 ± 5 nm. After spin-coating the solution, Au or LiF/Al was deposited on top of the blend film under vacuum. The hole and electron carrier mobilities were determined using the modified Mott-

Gurney equation, $J = (9/8)\varepsilon_0\varepsilon_r\mu(V^2/L^3)$, where J is the current density, μ is the mobility, and V is the applied voltage, and the device thickness, L, is defined. ε_0 is the vacuum permittivity and ε_r is the relative permittivity.[33]

Result and discussion

Synthesis of a regioisomeric PT-based conjugated polymer

To demonstrate the feasibility of conjugated terpolymers as p-type materials in BHJ-type PSCs, we synthesized three new PT derivative polymers; **Reg-BT**, **Ran-TT**, and **Reg-TT**. The **Ran-BT** was synthesized as a control polymer.[34,35] Detailed procedures for the synthesis of the monomers and polymers are depicted in **Scheme 1**. By employing the terpolymer structure and tuning the structural regularity of the polymer backbone, numerous attempts were made to find PT-based analogues with the optimal structure for PSCs. First, the CT unit in the repeating group of **Ran-TT** was arranged randomly. **Reg-TT** was also synthesized to regulate the arrangement of the CT monomeric unit in a regio-regular manner. The TT moiety was then introduced in a periodic fashion to increase the planarity and rigidity in the direction of the polymer chain. For TT-containing polymers, intermolecular interactions between the polymer chains should be enhanced with increasing crystallinity. As shown in **Scheme 1**, the binary copolymers (**Ran-BT** and **Reg-BT**) and regular terpolymers (**Ran-TT** and **Reg-TT**) were prepared through the Stille coupling reaction using a Pd-catalyst (e.g. $Pd_2(dba)_3$) and $P(o\text{-tolyl})_3$ as a ligand. The terpolymer **Ran-TT** was prepared by polymerizing **3**, **M3**, and **M4** in toluene at 110 °C. **Reg-TT** was also prepared from **7** and **M4** in toluene at 110 °C. The control polymer **Ran-BT** was synthesized from **3** and **M3** through the same coupling reaction, while **Reg-BT** was prepared from **7** and **M3**. The obtained crude polymers were purified by successive Soxhlet extraction with acetone, hexane, dichloromethane, and chloroform. After concentrating the chloroform solution, reprecipitation was performed in methanol. The molecular weights and polydispersity indices (PDIs) of the polymers were measured by gel permeation chromatography (GPC) using 1,2-dichlorobenzene (*o*-DCB) as the solvent. The number average molecular weights (M_n) of **Ran-TT**, **Reg-TT**, **Ran-BT**, and **Reg-BT** were 33.8, 23.5, 12.3, and 32.4 kDa, and the PDIs were 2.01, 2.24, 1.86, and 1.97, respectively. Even though **Ran-TT** and **Reg-TT** have the same backbone, they differ significantly in terms of the regularity of the arrangement of the CT monomer, thus their solubility will differ due to the difference in the polymer structure. **Reg-TT** has a relatively high degree of crystallinity due to the rigid and planar repeating unit

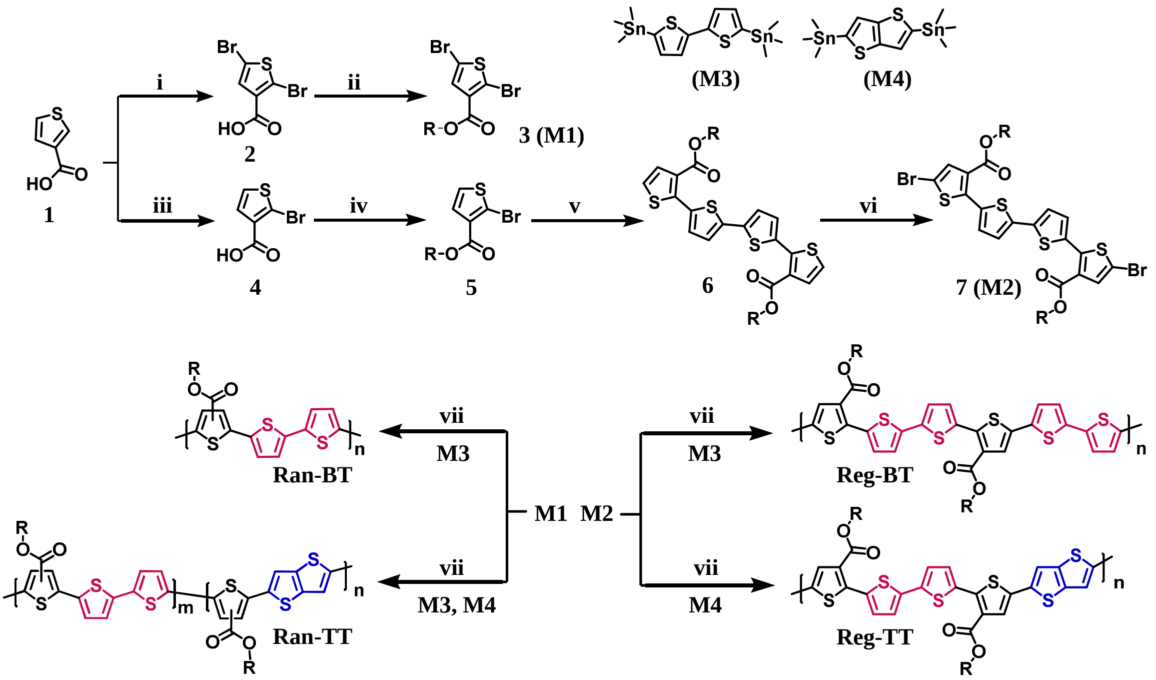

Scheme 1. Synthetic procedure of monomers and polymers. (i) Br_2, AcOH; (ii) 1-iodo-2-hexyldecane, K_2CO_3, DMF; (iii) *n*-BuLi, Br_2, THF; (iv) 1-iodo-2-hexyldecane, K_2CO_3, DMF; (v) **M3**, $Pd_2(dba)_3$, P(*o*-tolyl)$_3$, toluene/DMF (9:1 v/v); (vi) NBS, chloroform/AcOH (1:1 v/v); (vii) $Pd_2(dba)_3$, P(*o*-tolyl)$_3$, toluene. (R = 2-hexyldecyl).

structure and the strong intermolecular interactions between the polymer chains.(**Fig. S8**) Therefore, it is expected to show poor solubility in various organic solvents. Moreover, during fabrication of the blend film with ITIC, large polymer domains may be formed. A regular terpolymer system was introduced to resolve the disadvantages of **Ran-BT** and **Reg-BT**, providing a regular monomer arrangement composed of two monomeric units. This terpolymer system may provide an avenue for modifying various physical properties of the polymer, such as the solubility, thermal properties, and crystallinity, by changing the type of repeating unit and thus the conjugative effect.[36,37]

Thermal properties

Differential scanning calorimetry (DSC) thermograms were recorded to observe the thermal transition behavior of the synthesized polymers. The thermal properties of conjugated polymers are important factors that can be used to predict the thermal stability of the organic

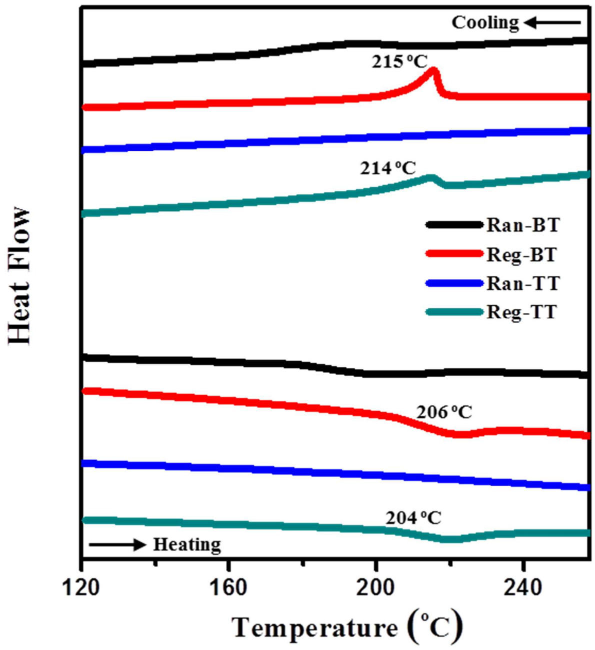

Fig. 1. DSC thermograms of **Ran-BT**, **Reg-BT**, **Ran-TT**, and **Reg-TT**

semiconductor devices in which they are employed. For **Reg-BT** and **Reg-TT** polymers, the glass transition temperatures were 206 °C and 204 °C, respectively, as reproducibly confirmed in the cooling cycle. In addition, no melting of the polymers was observed between 25 °C and 330 °C, and no thermal decomposition was observed. The cold crystallization temperatures (T_c) of **Reg-BT** and **Reg-TT** were observed at 215 °C and 214 °C, respectively, as indicated by clear T_c peaks, attributed to the rigid, regular backbone, in contrast to the **Ran-BT** and **Ran-TT** polymers.[38,39]

Optical and electrochemical properties

To investigate the optical properties of the synthesized PT derivatives and the ITIC acceptor, UV-vis absorption spectra were acquired in chloroform (CF) solution and in the film state. The data is summarized in **Table 1**. The absorption wavelength range for the PT derivatives, **Ran-BT**, **Reg-BT**, **Reg-TT**, and **Ran-TT,** was complementary to the absorption range of ITIC and spanned the range of 300−650 nm for the blend films. Generally, the absorption spectrum of a regio-regular conjugated polymer in the solution state is red-shifted and much

Table 1. Optical and electrochemical properties of **Ran-BT**, **Reg-BT**, **Ran-TT**, **Reg-TT**, and ITIC.

Polymer	M_n (kDa)	PDI	λ_{peak}^a (nm)	λ_{peak}^b (nm)	λ_{edge}^c (nm)	$E_g^{opt,d}$ (eV)	E_{ox}^{onset} (V)	E_{red}^{onset} (V)	Energy Level (eV)	
									HOMO[e]	LUMO[e]
Ran-BT	12.3	1.86	493	552	651	1.90	0.78	-	-5.23	-3.33
Reg-BT	32.4	1.97	519	557	649	1.91	0.82	-	-5.27	-3.34
Ran-TT	33.8	2.01	539	552	640	1.94	0.89	-	-5.34	-3.40
Reg-TT	23.5	2.24	555	558	648	1.91	0.84	-	-5.29	-3.38
ITIC	-	-	678	700	766	1.62	-	-0.45	-5.63	-4.00

[a] chloroform solution, [b] film, [c] Absorption edge of the polymer films. [d] Calculated from the absorption edge of the polymer films: $E_g^{opt} = 1240 / \lambda_{edge}$, [e] Calculated according to the equation $E_{HOMO/LUMO} = -e\ (E_{ox/red} + 4.40)$ (eV).

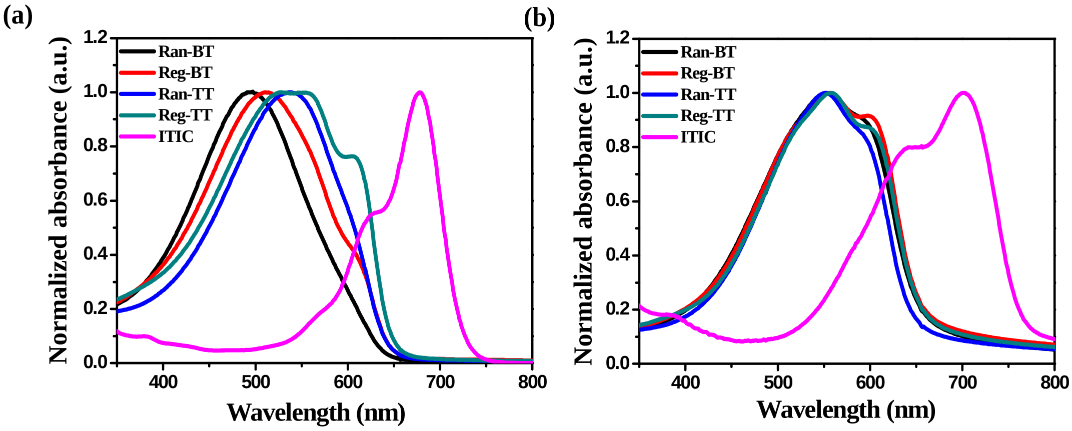

Fig. 2. Normalized optical absorption spectra of **Ran-BT**, **Reg-BT**, **Ran-TT**, **Reg-TT** and ITIC (a) in chloroform solution and (b) in the as-cast film states.

wider than that of a regio-random conjugated polymer. This suggests that regio-regular conjugated polymers have a well-ordered, uniform monomer arrangement with strong intermolecular interactions between the polymer chains.[40]

Interestingly, in the spectra of the regio-regular copolymers, **Reg-BT** and **Reg-TT**, shoulder peaks were observed at a wavelength of 608 nm. These were attributed to the strong intermolecular interactions arising from the regularity of the polymer backbones. However, as shown in **Fig. 2b**, all four polymers exhibited similar absorption peaks in the film form. In the polymer film state, it is common to observe absorption at longer wavelengths due to intermolecular interactions, as opposed to in the solution state. The profiles of **Ran-BT**, **Reg-BT**, **Ran-TT**, and **Reg-TT** displayed spectral red-shifts of 59, 38, 13, and 3 nm, respectively, and the maximum absorption was observed at 555−560 nm for all polymers. For the solution-state absorption spectrum, the shoulder peak at 600 nm was still observed in the film state.[41]

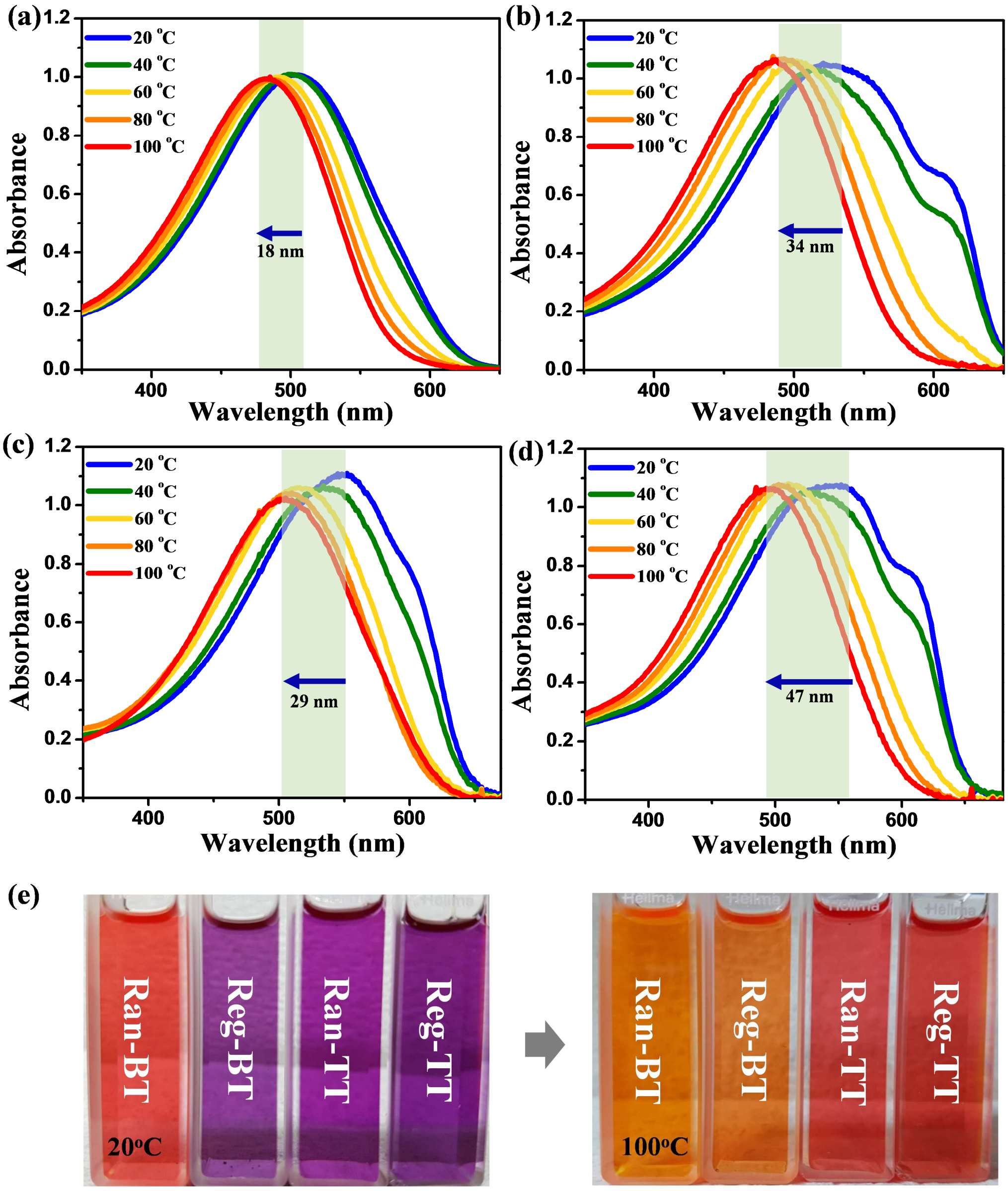

Fig. 3. Temperature-dependent absorption (TD-Abs) of the four polymers in chlorobenzene solution: (a) **Ran-BT**, (b) **Reg-BT**, (c) **Ran-TT**, (d) **Reg-TT**, and (e) photographic images of the four polymer solutions taken at 20 °C and 100 °C.

The aggregation behavior of the four polymers in chlorobenzene (CB) solution was investigated via UV-vis absorption spectroscopy while varying the solution temperature. Generally, as the solution temperature increased, regio-regular polymers (**Fig. 3b** and 3**d**) showed a much larger hypochromic shift compared to regio-random polymers (**Fig. 3a** and **3c**). This is because the regio-regular polymer undergoes aggregation, even in solution. When the temperature was increased, the intermolecular interactions were weakened and the spectrum was shifted to the short wavelength region. Because the interaction between the main chains can be reduced by increasing the temperature, the main absorption peak is due to an intramolecular π-π^* transition.[42]

Compared with binary copolymers (e.g. **Ran-BT** and **Reg-BT**; **Fig. 3a** and **3b**), terpolymers with the TT moiety (e.g. **Ran-TT** and **Reg-TT**) (**Fig. 3c** and **3d**) showed stronger interchain interactions, allowing the difference between the regio-random and regio-regular polymers to be investigated in terms of the interchain interactions of the binary copolymer and terpolymer. Based on these results, it was confirmed that the intermolecular interactions in the regio-regular polymer were more effective than in the regio-random polymer, as predicted.[43]

Electrochemical cyclic voltammetry (CV) was performed to investigate the HOMO and LUMO energy levels of the conjugated polymers. All CV measurements were performed in a solution of 0.1 M Bu_4NPF_6 in acetonitrile. The oxidation and reduction potentials were calibrated using the ferrocene/ferrocenium (Fc/Fc^+) redox couple and the electrochemical parameters of the **Ran-BT**, **Reg-BT**, **Ran-TT**, **Reg-TT,** and ITIC films on a Pt electrode are summarized in **Table 1**. Detailed CV data and energy levels are summarized in **Fig. S2**. The HOMO energy levels of **Ran-BT**, **Reg-BT**, **Ran-TT**, **Reg-TT,** and ITIC were -5.23, -5.27, -5.34, -5.29, and -5.63 eV, respectively, and the corresponding LUMO energy levels were calculated to be -3.33, -3.34, -3.40, -3.38, and -4.00 eV, respectively. The terpolymers, **Ran-TT** and **Reg-TT,** have lower-lying HOMO energy levels than do the binary copolymer systems, with **Ran-TT** having the lowest HOMO energy value (-5.34 eV). The PSC prepared using **Ran-TT** as the donor polymer and ITIC as the acceptor should have a relatively high V_{oc}.

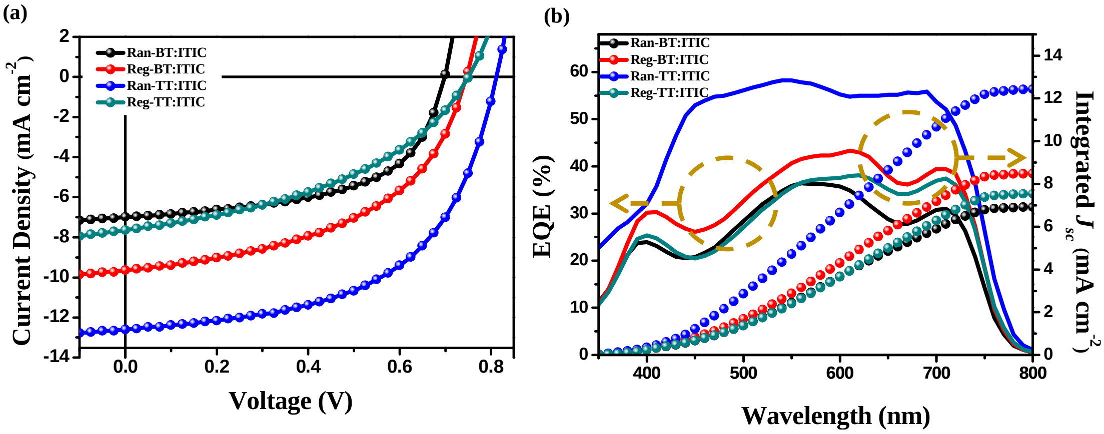

Fig. 4. (a) Representative *J-V* characteristics and (b) external quantum efficiency (EQE) spectra and integrated J_{sc} of BHJ-PSC devices using the polymer:ITIC blend films (1:1, w/w ; annealed at 100 ^{o}C for 10 min) as the active layer.

Performance of PSCs with ITIC

To investigate the influence of the regio-regularity and terpolymer structure on the photovoltaic performance of the PT derivatives, PSC devices were fabricated with an inverted device structure: ITO/ZnO (30 nm)/BHJ active layer/MoO_3 (10 nm)/Ag (100 nm), where the polymers **Ran-BT**, **Reg-BT**, **Ran-TT**, and **Reg-TT** were used as electron donors and ITIC was used as a fullerene-free acceptor. The blend composition was optimized with a 1:1 donor/ITIC weight ratio. The blend film made using chloroform exhibited the best performance in the PSCs. **Fig. 4a** shows the current-density versus voltage (*J*−*V*) curves measured under AM 1.5 G illumination (100 mW cm^{-2}). Representative characteristics of the inverted PSCs, such as the V_{oc}, J_{sc}, fill factor (FF), and PCE, are summarized in **Table 2**. The device fabricated with **Ran-BT** in the absence of any solvent additive showed a V_{oc} of 0.70 V, a J_{sc} of 6.98 mA cm^{-2}, an FF of 56.5%, and a PCE of 2.75%. The device with **Reg-BT** exhibited a V_{oc} of 0.72 V, a J_{sc} of 8.57 mA cm^{-2}, an FF of 43.7%, and a PCE of 2.70%. Due to the high crystallinity of **Reg-BT**, the FF was lowered while the V_{oc} and J_{sc} increased slightly, resulting in unprecedentedly similar PCEs. The devices made with **Ran-TT** and **Reg-TT** displayed a V_{oc} of 0.81 and 0.75 V, J_{sc} of 12.57 and 7.62 mA cm^{-2}, FF of 55.3 and 42.6%, and PCE of 5.65 and 2.43%, respectively. Although three of the polymers showed similar efficiencies, it is noteworthy that the J_{sc} of the device fabricated with **Ran-TT** was almost twice as high as that of the other polymers, giving the best efficiency.

In order to observe the characteristics of the PSC manufactured in this study more closely, the device was fabricated under various conditions to obtain the J-V curves (**Fig. S3-S6**) and the photovoltaic parameters (**Table S1-S4**) were shown in the support information. The data in **Table S1** demonstrates that the PSC devices fabricated using CB as a solvent had relatively low FF, J_{sc}, and PCE values compared to the devices made by employing CF as a solvent. However, same tendency could be observed that regio-random polymer based PSCs displayed higher performance than the devices with regio-regular polymers. In brief, the BHJ photovoltaic performance of **Ran-TT** based PSC was superior to that of the other polymers.

The **Ran-TT**:ITIC blend active layer showed the highest PCE of 5.32% without thermal annealing. For the PSC fabricated by thermal annealing at 100 °C for modification of the internal structure of the active layer, the FF increased and the measured PCE was 5.65%, which is higher than that without thermal annealing. The high J_{sc} value of the PSC was confirmed by external quantum efficiency (EQE) spectroscopy (**Fig. 4b**). As predicted, the EQE spectrum generally matched the light absorption spectrum of the corresponding blend films for the active layers. The integrated J_{sc} values of the devices are well consistent with those obtained from **Fig. 4b.** The EQE spectra of all blend films showed a broad, strong band in the 300−800 nm region due to the complementarity between the absorption spectra of the PT derivatives and ITIC. The maximum EQE values of the PSCs based on **Ran-BT**, **Reg-BT**, **Ran-TT**, and **Reg-TT** were 36, 42, 58, and 37%, respectively. The highest EQE values observed with the **Ran-TT**-based PSCs indicated highly efficient photon and charge collection in the active layer.

Table 2. Photovoltaic properties of PSCs made from chloroform solution with a ITO/ZnO/polymer:ITIC (1:1, w/w)/MoO_3/Ag device structure measured under AM 1.5G illumination (100 mW cm^{-2}); The active layers were annealed at 100 ^{o}C for 10 min.

Donor	Acceptor	V_{oc} (V)	J_{sc} (mA cm^{-2})	FF (%)	PCE (%)	Integrated J_{sc} (mA cm^{-2})
Ran-BT	**ITIC**	0.70 (0.71±0.01)	6.98 (6.93 ±0.05)	56.5 (51.2±5.30)	2.75 (2.65±0.10)	6.93
Reg-BT		0.72 (0.73±0.01)	8.57 (8.12±0.45)	43.7 (40.9±2.10)	2.70 (2.44±0.26)	8.49
Ran-TT		0.81 (0.80±0.01)	12.63 (11.72±0.91)	55.3 (52.2±3.10)	5.65 (4.98±0.67)	12.46
Reg-TT		0.75 (0.74±0.01)	7.62 (7.33±0.29)	42.6 (39.9±2.65)	2.43 (2.15±0.28)	7.55

Average values and standard deviations were obtained from more than 10 devices. They are in parentheses.

We also investigated the charge mobilities of the single carrier devices such as hole-only device (HOD) and electron-only device (EOD) to understand the different PSC performance described above. The hole and electron mobilities of the blend films were measured using the space-charge limited current (SCLC) method. HOD and EOD properties were summarized in **Fig. S7** and **Table S5.** Compared to the blends film of regio-regular polymers (e.g. **Reg-BT** and **Reg-TT**) and ITIC, the blend films of regio-random polymers and ITIC exhibited better hole and electron charge balance, which may contribute to the higher FF values of the corresponding PSCs.[44,45] In particular, **Reg-TT**:**ITIC** blend film displays the worst charge mobility balance, resulting in the lowest PCE in the corresponding PSC.

Morphological studies of the blend film of the polymer and ITIC

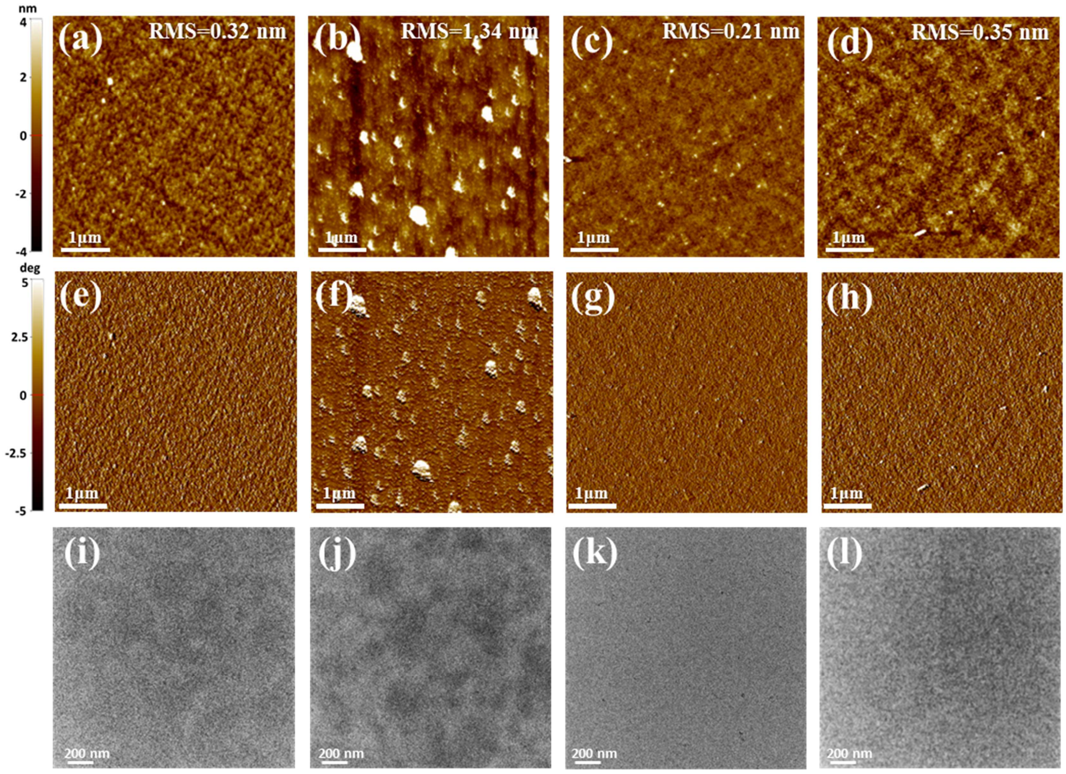

Fig. 5. (a−d) AFM height images, (e−h) phase images, and (i−l) TEM images of polymer:ITIC (1:1) blend films. **Ran-BT**:ITIC (a, e, i), **Reg-BT**:ITIC (b, f, j), **Ran-TT**:ITIC (c, g, k), **Reg-TT**:ITIC (d, h, l); all samples were annealed at 100 ^{o}C for 10 min.

Atomic force microscopy (AFM) and transmission electron microscopy (TEM) were employed to investigate the internal and surface morphology of the polymer:ITIC blend films prepared from chloroform after annealing at 100 °C for 10 min.[46]

Fig. 5a−h shows height and phase images of the optimized blend films obtained using AFM. Overall, the regio-random polymers (e.g. **Ran-BT** and **Ran-TT**) showed a finer morphology than the regio-regular polymers (**Reg-BT** and **Reg-TT**). The images of **Reg-BT** in **Fig. 5b** and **f** show a very coarse surface with a high root-mean-square (RMS) roughness, which was attributed to severe aggregation due to the unique structure of the polymer. In contrast, the images of **Ran-TT** in **Fig. 5c** and **g** show desirably fine phase separation and a highly homogeneous interpenetrating network, which is beneficial for exciton diffusion/dissociation and charge carrier transport, and a low RMS roughness value.[47] It was deduced that the suitable morphology of the **Ran-TT**:ITIC film lead to PSCs with relatively high performance.

TEM measurements were performed to monitor the internal morphology of the four polymers and ITIC mixtures prepared under optimal conditions. As shown in **Fig. 5i−l**, the internal morphology of **Reg-BT** comprised large aggregates, similar to those observed in the AFM surface images. In contrast, the fine internal morphology of the **Ran-TT** films was observed. The latter is much more advantageous for exciton diffusion, charge separation, and charge transport within the active layer of the PSC due to the effective formation of small charge migration channels. These results explained the higher J_{sc} values of the **Ran-TT**:ITIC-based PSC relative to those of the PSCs employing the other polymers.

Conclusion

In conclusion, we successfully synthesized two regioisomeric π-conjugated terpolymers bearing thiophene carboxylate, bithiophene, and thienothiophene (e.g. **Ran-TT** and **Reg-TT**). Conjugated polymers with thiophene carboxylate showed significant differences in their absorption properties, HOMO / LUMO energy levels, and bandgap compared to polythiophene only with neat thiophene. This study confirmed that the characteristics of binary conjugated copolymers can be tuned by synthesizing conjugated terpolymers with a third monomer (e.g. TT) in the repeating group. Regio-regular and regio-random terpolymers also displayed different absorption properties and HOMO / LUMO energy levels. Of the four polymers synthesized, the **Ran-TT** terpolymer exhibited a lower-lying HOMO level (-5.34 eV) than conventional polythiophene derivatives, and was expected to show a higher V_{oc} value in the corresponding BHJ-type PSCs.

Among the PSC devices fabricated in this study, the **Ran-TT**:ITIC-based PSC exhibited the highest PCE of 5.65% with a high short circuit current density of 12.63 mA cm^{-2} and an open circuit voltage of 0.81 V. The results of this study confirmed that the internal morphology of the blend films of ITIC and regio-random terpolymer facilitated exciton diffusion and charge migration, in contrast to that of regio-regular polymer-based blend films. This gives a higher short circuit current density, which is advantageous for increasing the efficiency of the PSC.

Acknowldgements

This research was supported by the National Research Foundation of Korea (NRF2015R1A2A1A05001876) and by the Key Research Institute Program (NRF20100020209). We are grateful to Pohang Accelerator Laboratory (Pohang, Korea) for allowing us to conduct the grazing incidence wide angle X-ray diffraction (GIWAXD) measurements.

References

[1] W. Zhao, D. Qian, S. Zhang, S. Li, O. Inganas, F. Gao, J. Hou, Fullerene-free polymer solar cells with over 11% efficiency and excellent thermal stability, Adv. Mater. 28 (2016) 4734–4739.

[2] G. Zhang, G. Yang, J.-H. Kim, H. Ade, W. Wu, X. Xu, Y. Duan, Q. Peng, Effcient nonfullerene polymer solar cells enabled by a novel wide bandgap small molecular acceptor, Adv. Mater. 29 (2017) 1606054.

[3] F. Zhao, S. Dai, Y. Wu, Q. Zhang, J. Wang, L. Jiang, Q. Ling, Z. Wei, W. Ma, W. You, C. Wang, X. Zhan, Single-junction binary-blend nonfullerene polymer solar cells with 12.1% effciency, Adv. Mater. 29 (2017) 1700144.

[4] A. J. Heeger, 25th Anniversary Article: Bulk heterojunction solar cells: understanding the mechanism of operation, Adv. Mater. 26 (2014) 10–28.

[5] G. Yu, J. Gao, J. C. Hummelen, F. Wudl, A. J. Heeger, Polymer photovoltaic cells: enhanced efficiencies via a network of internal donor-acceptor heterojunctions, Science 270 (1995) 1789–1791.

[6] G. Li, R. Zui, Y. Yang, Polymer solar cells, Nature Photon. 6 (2012) 153–161.

[7] S. Li, L. Ye, W. Zhao, S. Zhang, S. Mukherjee, H. Ade, J. Hou, Energy-level modulation of small-molecule electron acceptors to achieve over 12% effciency in polymer solar cells, Adv. Mater. 28 (2016) 9423–9429.

[8] W. Chen, Q. Zhang, Recent progress in non-fullerene small molecule acceptors in organic solar cells (OSCs), J. Mater. Chem. C 5 (2017) 1275–1302.

[9] N. Liang, W. Jiang, J. Hou, Z. Wang, New developments in non-fullerene small molecule acceptors for polymer solar cells, Mater. Chem. Front. 1 (2017) 1291–1303.

[10] S. M. McAfee, J. M. Topple, I. G. Hill, G. C. Welch, Key components to the recent performance increases of solution processed non-fullerene small molecule acceptors, J. Mater. Chem. A 3 (2015) 16393–16408.

[11] Y. Z. Lin, J. Y. Wang, Z. G. Zhang, H. T. Bai, Y. F. Li, D. B. Zhu, X. W. Zhan, An electron acceptor challenging fullerenes for efficient polymer solar cells, Adv. Mater. 27 (2015) 1170–1174.

[12] D. P. Qian, L. Ye, M. J. Zhang, Y. R. Liang, L. J. Li, Y. Huang, X. Guo, S. Q. Zhang, Z. A. Tan, J. Hou, Design, application, and morphology study of a new photovoltaic polymer with strong aggregation in solution state, Macromolecules 45 (2012) 9611–9617.

[13] J. Hou, T. L. Chen, S. Zhang, L. Huo, S. Sista, Y. Yang, An easy and effective method to modulate molecular energy level of poly(3-alkylthiophene) for high-V_{oc} polymer solar cells, Macromolecules 42 (2009) 9217–9219.

[14] S. Gunes, H. Neugebauer, N. S. Sariciftci, Conjugated polymer-based organic solar cells, Chem. Rev. 107 (2007) 1324–1338.

[15] Y. J. Cheng, S. H. Yang, C. S. Hsu, Synthesis of conjugated polymers for organic solar cell applications, Chem. Rev. 109 (2009) 5868–5923.

[16] E. Zhou, Z. Tan, Y. Yang, L. Huo, Y. Zou, C. Yang, Y. Li, Synthesis, hole mobility, and photovoltaic properties of cross-linked polythiophenes with vinylene-terthiophene-vinylene as conjugated bridge, Macromolecules 40 (2007) 1831–1837.

[17] H. Xin, F. S. Kim, S. A. Jenekhe, Highly efficient solar cells based on poly(3-butylthiophene) nanowires, J. Am. Chem. Soc. 130 (2008) 5424–5425.

[18] K. H. Hendriks, G. H. L. Heintges, V. S. Gevaerts, M. M. Wienk, R. A. J. Janssen, High-molecular-weight regular alternating diketopyrrolopyrrolebased terpolymers for efficient organic solar cells, Angew. Chem. Int. Ed. 52 (2013) 8341–8344.

[19] M. Zhang, X. Guo, Y. Yang, J. Zhang, Z.-G. Zhang, Y. Li, Downwards tuning the HOMO level of polythiophene by carboxylate substitution for high open-circuit-voltage polymer solar cells, Polym. Chem. 2 (2011) 2900–2906.

[20] M. Zhang, X. Guo, W. Ma, H. Ade, J. Hou, A polythiophene derivative with superior properties for practical application in polymer solar cells, Adv. Mater. 26 (2014) 5880–5885.

[21] Y. Qin, M. A. Uddin, Y. Chen, B. Jang, K. Zhao, Z. Zheng, R. Yu, T. J. Shin, H. Y. Woo, J. Hou, Highly effcient fullerene-free polymer solar cells fabricated with polythiophene derivative, Adv. Mater. 28 (2016) 9416–9422.

[22] H. Bin, Z. G. Zhang, L. Gao, S. Chen, L. Zhong, L. Xue, C. Yang, Y. F. Li, Non-fullerene polymer solar cells based on alkylthio and fluorine substituted 2D-conjugated polymers reach 9.5% efficiency, J. Am. Chem. Soc. 138 (2016) 4657–4664.

[23] Y. J. Cheng, S. H. Yang, C. S. Hsu, Synthesis of conjugated polymers for organic solar cell applications, Chem. Rev. 109 (2009) 5868–5923.

[24] W. Li, K. H. Hendriks. A. Furlan, A. Zhang, M. M Wienk, R. A. J. Janssen, A regioregular terpolymer comprising two electron-deficient and one electron-rich unit for ultra small band gap solar cells, Chem. Commun, 51 (2015) 4290–4293.

[25] T. Qin, W. Zajaczkowski, W. Pisula, M. Baumgarten, M. Chen, M. Gao, G. Wilson, C. D. Easton, K. Müllen and S. E. Watkins, Tailored donor-acceptor polymers with an A-D1-A-D2 structure: controlling intermolecular interactions to enable enhanced polymer photovoltaic devices, J. Am. Chem. Soc. 136 (2014) 6049–6055.

[26] W. Sun, Z. Ma, D. Dang, W. Zhu, M. R. Andersson, F. Zhang and E. Wang, An alternating D–A1–D–A2 copolymer containing two electron-deficient moieties for efficient polymer solar cells, J. Mater. Chem. A 1 (2013) 11141–11144.

[27] W. A. Braunecker, S. D. Oosterhout, Z. R. Owczarczyk, N. Kopidakis, E. L. Ratcliff, D. S. Ginley, D. C. Olson, Semi-random vs well-defined alternating donor-acceptor copolymers, ACS Macro Lett. 3 (2014) 622–627.

[28] Z. Deng, L. Chen and Y. Chen, Novel phenanthrocarbazole based donor–acceptor random and alternating copolymers for photovoltaics, J. Polym. Sci., Part A: Polym. Chem. 51 (2013) 4885–4893.

[29] Y. Otaki, Y. Miyagi, F. Sanda, Synthesis and properties of novel optically active poly(thiophenyleneethynylene-phenyleneethynylene)s, Chem. Lett. 44 (2015) 1013–1015.

[30] M. Pomerantz, A. S. Amarasekara, H. V. R. Dias, Synthesis and solid-state structures of dimethyl 2,2′-bithiophenedicarboxylates, J. Org. Chem. 67 (2002) 6931–6937.

[31] J-C Ribierre, L. Zhao, M. Inoue, P-O. Schwartz, J-H. Kim, K. Yoshida, A. S. D. Sandanayaka, H. Nakanotani, L. Mager, S. Mercy, C. Adachi, Low threshold amplified spontaneous emission and ambipolar charge transport in non-volatile liquid fluorene derivatives, Chem. Commun. 52 (2016) 3103–3106.

[32] W. Wang, B. Zhao, H. Wu, Z. Guo, Y. Mi, Z. Zhang, C. Gao, Z. An, Synthesis of a low bandgap polymer based on thieno[3,2-b]thiophene and fluorinated quinoxaline derivatives and its application in bulk heterojunction solar cells, Synth. Met. 206 (2015) 66–71.

[33] J. A. Rohr, D. Moia, S. A. Haque, T. Kirchartz, J. Nelson, Exploring the validity and limitations of the Mott-Gurney law for charge-carrier mobility determination of semiconducting thin-films, J. Phys.: Condens. Matter 30 (2018) 105901

[34] P. Deng, B. Wu, Y. Lei, H. Cao, B. S. Ong, Regioregular and random difluorobenzothiadiazole electron donor-acceptor polymer semiconductors for thin-film transistors and polymer solar cells, Macromolecules 49 (2016) 2541–2548.

[35] K. H. Hendriks, G. H. L. Heintges, M. M. Wienk, R. A. J. Janssen, Comparing random and regular diketopyrrolopyrrole–bithiophene–thienopyrrolodione terpolymers for organic photovoltaics, J. Mater. Chem. A 2 (2014) 17899–17905.

[36] E. Y. Ko, G. E. Park, D. H. Lee, H. A. Um, J. Shin, M. J. Cho, D. H. Choi, Enhanced performance of polymer solar cells comprising diketopyrrolopyrrole-based regular terpolymer bearing two different π-extended donor units, ACS. Appl. Mater. Interfaces 7 (2015) 28303–28310.

[37] M. L. Keshtov, A. R. Khokhlov, S. A. Kuklin, F. C. Chen, E. N. Koukaras, G. D. Sharma, New D-A1-D-A2-type regular terpolymers containing benzothiadiazole and benzotrithiophene acceptor units for photovoltaic application, ACS. Appl. Mater. Interfaces 8 (2016) 32998–33009.

[38] T. L. Nguyen, C. Lee, H. Kim, Y. Kim, W. Lee, J. H. Oh, B. J. Kim, H. Y. Woo, Ethanol-processable, highly crystalline conjugated polymers for eco-friendly fabrication of organic transistors and solar cells, Macromolecules 50 (2017) 4415–4424.

[39] S. Z. D. Cheng, X. X. Wu, A. Zhang, Thermal properties, phase transitions, and morphology of a conjugated polymer, Polym. Eng. Sci. 32 (1992) 1325–1332.

[40] H. Jiang, Z. Wang, L. Zhang, A. Zhong, X. Liu, F. Pan, W. Cai, O. Inganas, Y. Liu, J. Chen, Y. Cao, A highly crystalline wide-band-gap conjugated polymer toward high-performance as-cast nonfullerene polymer solar cells, ACS. Appl. Mater. Interfaces 9 (2017) 36061–36069.

[41] D. Beljonne, G. Pourtois, C. Silva, E. Hennebicq, L. M. Herz, R. H. Friend, G. D. Scholes, S. Setayesh, K. Müullen, J. L. Bredas, Interchain vs. intrachain energy transfer in acceptor capped conjugated polymers, PNAS 99 (2002) 10982–10987.

[42] S. Zhang, Y. Qin, M. A. Uddin, B. Jang, W. Zhao, D. Liu, H. Y. Woo, J. Hou, A fluorinated polythiophene derivative with stabilized backbone conformation for highly efficient fullerene and non-fullerene polymer solar cells, Macromolecules 49 (2016) 4415–4424.

[43] Y. Li, Y. Cao, J. Gao, D. Wang, G. Yu, A. J. Heeger, Electrochemical properties of luminescent polymers and polymer light-emitting electrochemical cells, Synth. Met. 99 (1999) 243–248.

[44] L. A. A. Pettersson, L. S. Roman, O. Inganas, Modeling photocurrent action spectra of photovoltaic devices based on organic thin films, J. Appl. Phys. 86 (1999) 487–496.

[45] D. Xia, Y. Wu, Q. Wang, A. Zhang, C. Li, Y. Lin, F. J. M. Colberts, J. J. V. Faneker, R. A. J. Janssen, X. Zhan, W. Hu, Z. Tang, W. Ma, W. Li, Effect of alkyl side chains of conjugated polymer donors on the device performance of non-fullerene solar cells, Macromolecules. 49 (2016) 6445–6454.

[46] S. H. Park, A. Roy, S. Beaupre, S. Cho, N. Coates, J. S. Moon, D. Moses, M. Leclerc, K. Lee, A. J. Heeger, Bulk heterojunction solar cells with internal quantum efficiency approaching 100%, Nature Photon. 3 (2009) 297–302.

[47] J. D. Miller, S. Veeramasuneni, J. Drelich, M. R. Yalamanchili, Effect of roughness as determined by atomic force microscopy on the wetting properties of PTFE thin films, Polym. Eng. Sci. 36 (1996) 1849–1855.

Highlight

1. Two regioisomeric π-conjugated terpolymers bearing carboxylated thiophene, thienothiophene and bithiophene (BT) were successfully synthesized.

2. The PSC with **Ran-TT** exhibited the highest power conversion efficiency of 5.65% with a high short circuit current density (J_{sc}) of 12.63 mA cm^{-2}.

3. The internal morphology of the **Ran-TT** was observed much more favorable than that of the regio-regular terpolymer for enhancing PSC performances.